A

A simplified diagram of how mTORC1 senses energy, growth factors, and amino acids

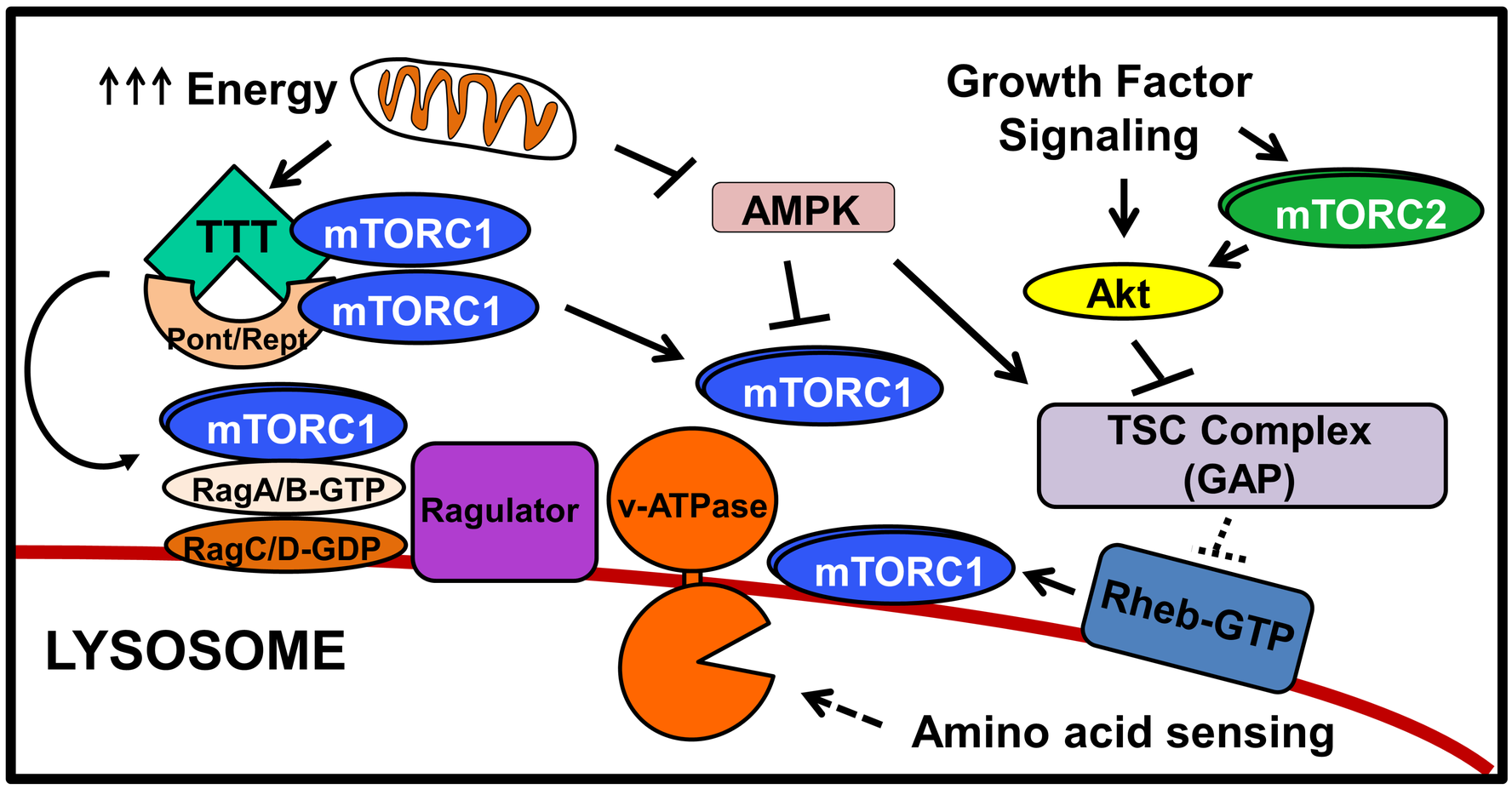

B

Retinal degeneration in *XE14C*

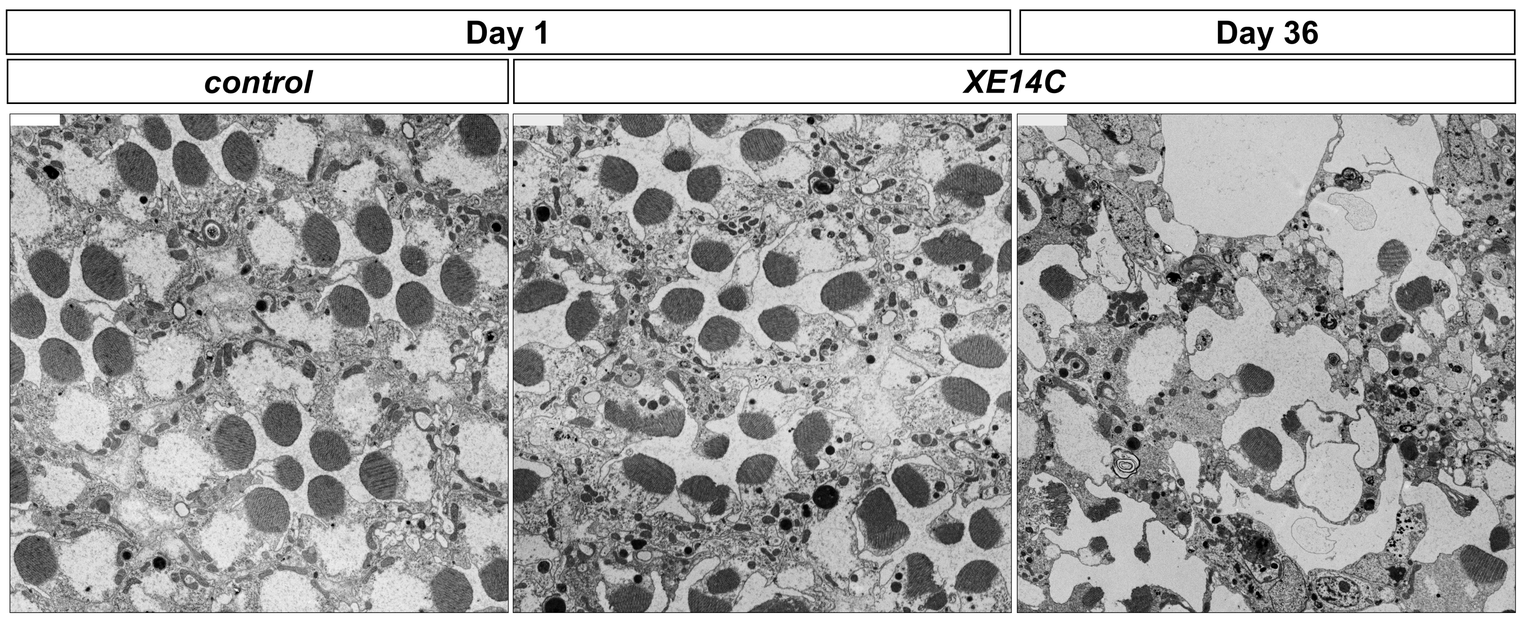

C

Increased autophagic vesicles in *XE14* mutant lamina

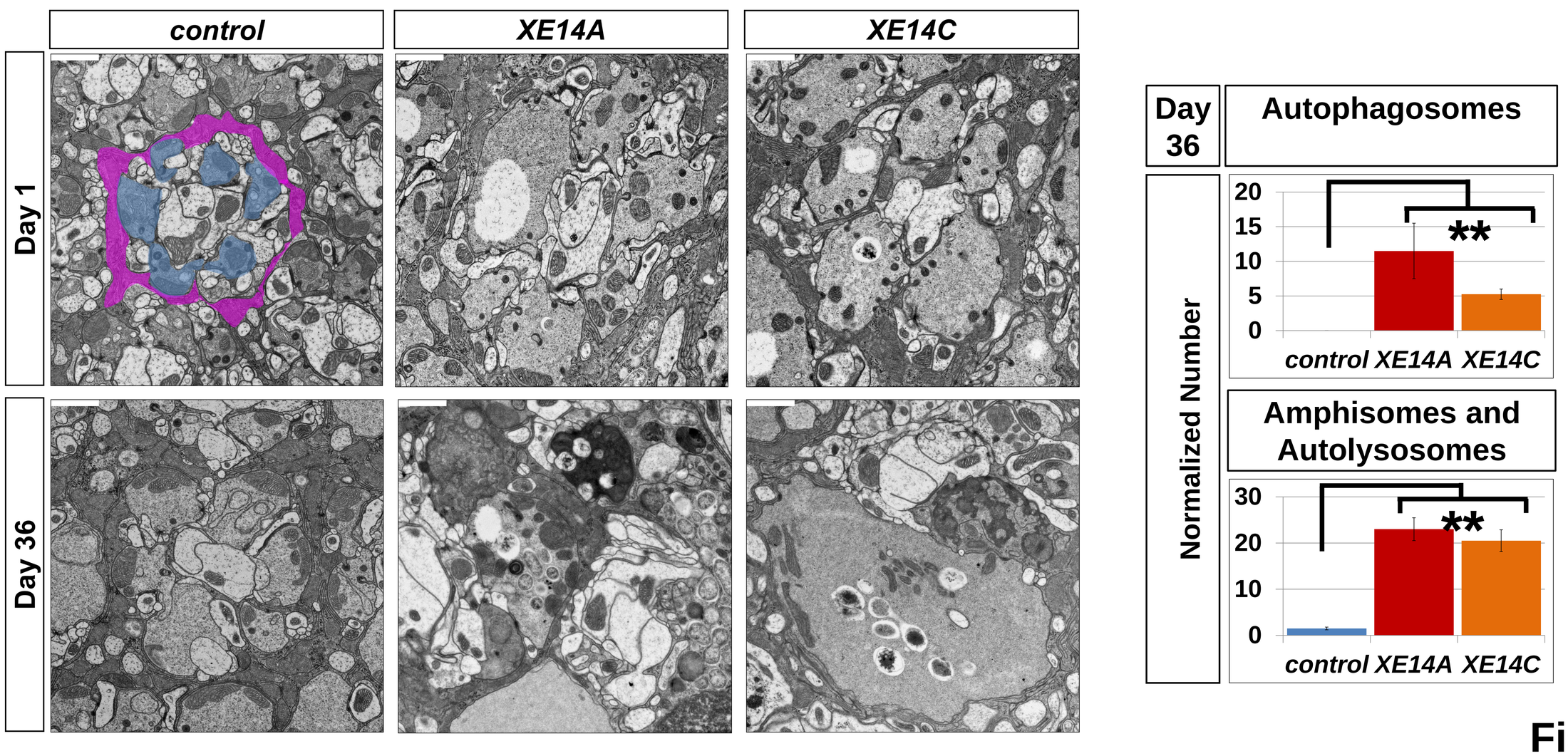

Figure S1

A

Genomic rescue of *wacky* retinal morphology

***wacky^{A}*, Day 5**	***wacky^{A}; wacky-gr*, Day 5**

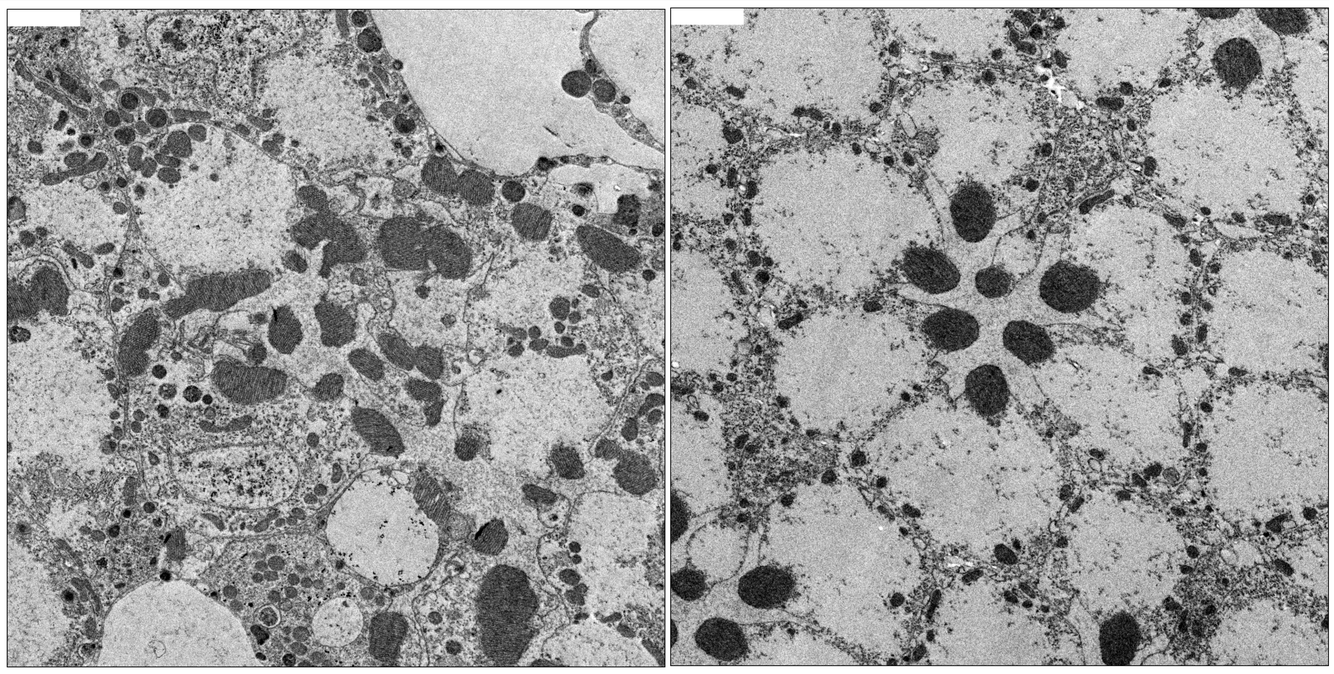

B Genomic rescue of *wacky* ERG defects

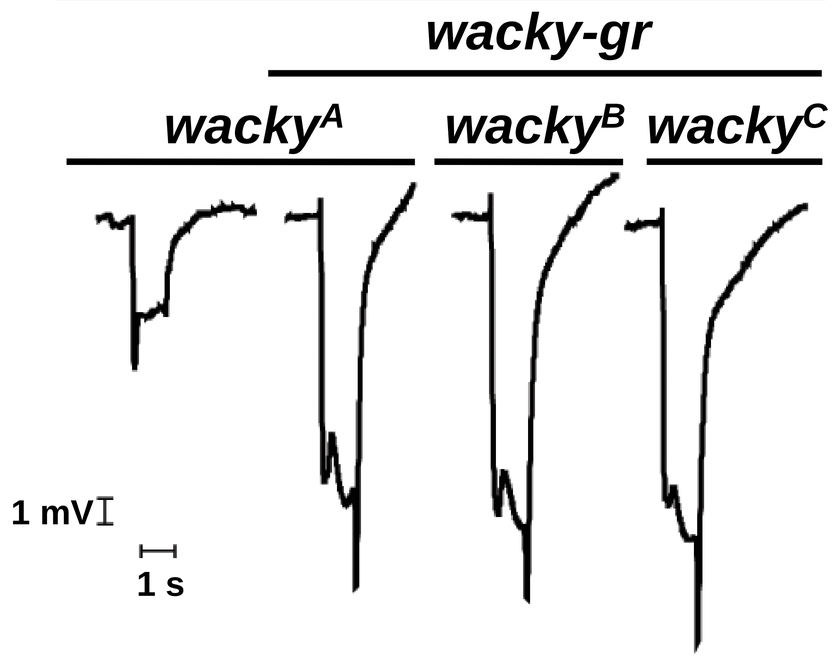

C Wacky is expressed in adult and larval tissue

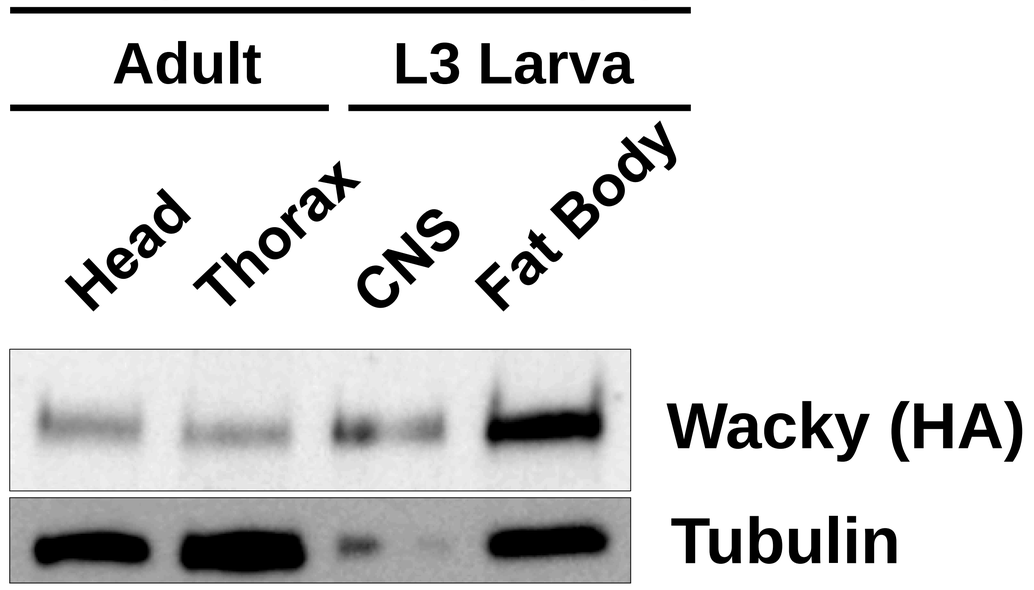

D Tagged Wacky genomic rescue construct is broadly expressed in larval tissues

***wacky^{C} ; 3F2H-wacky-gr*, L3 larva**			
eye disc	**wing disc**	**central brain**	**ventral nerve cord**

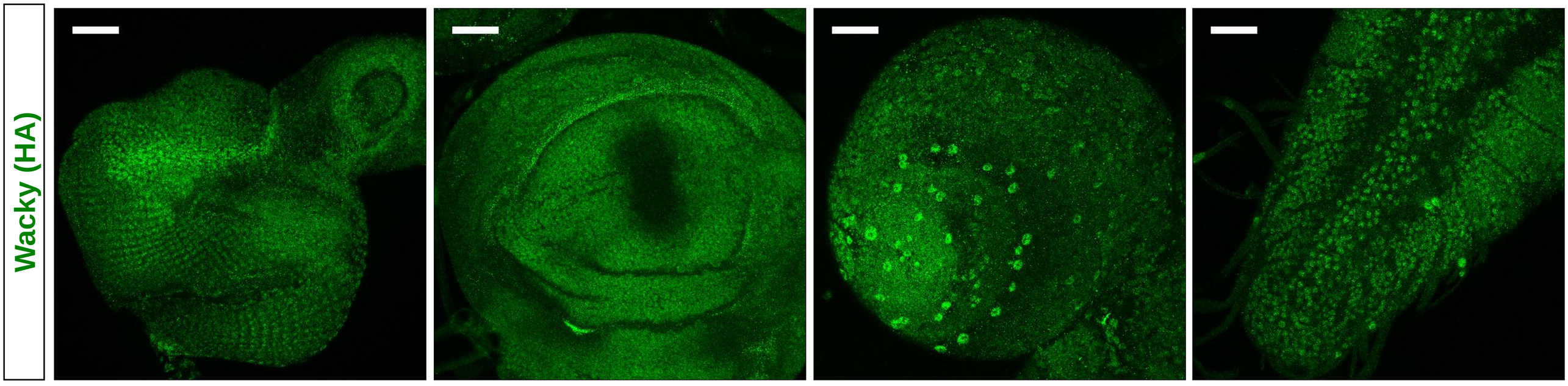

Figure S2

A Starvation-induced autophagy in wacky mutant clones

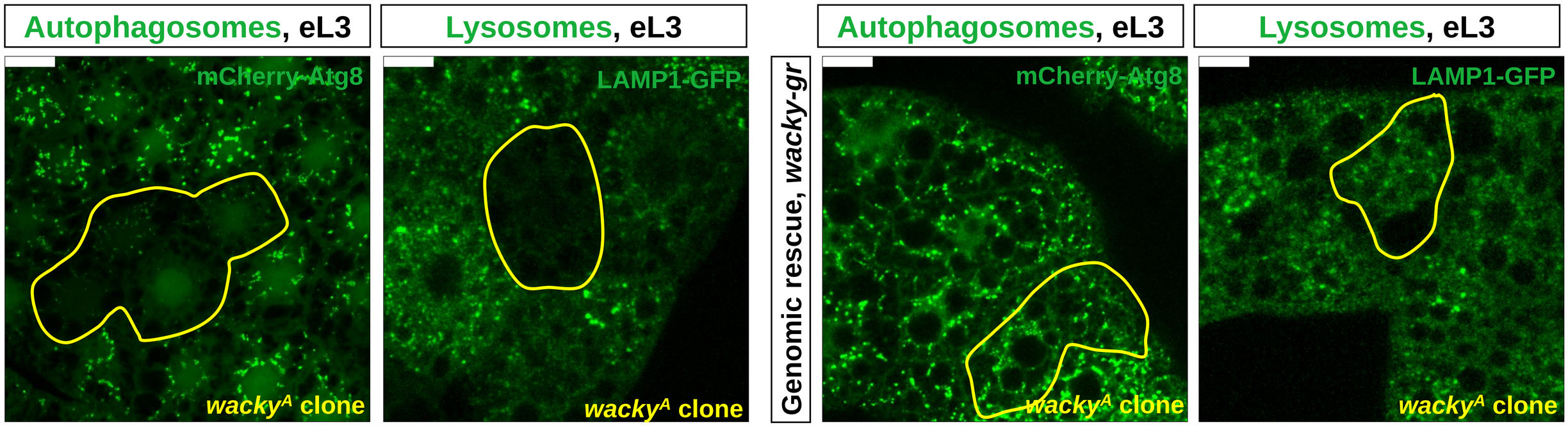

B Autophagosome-lysosome fusion occurs in *wacky* mutants

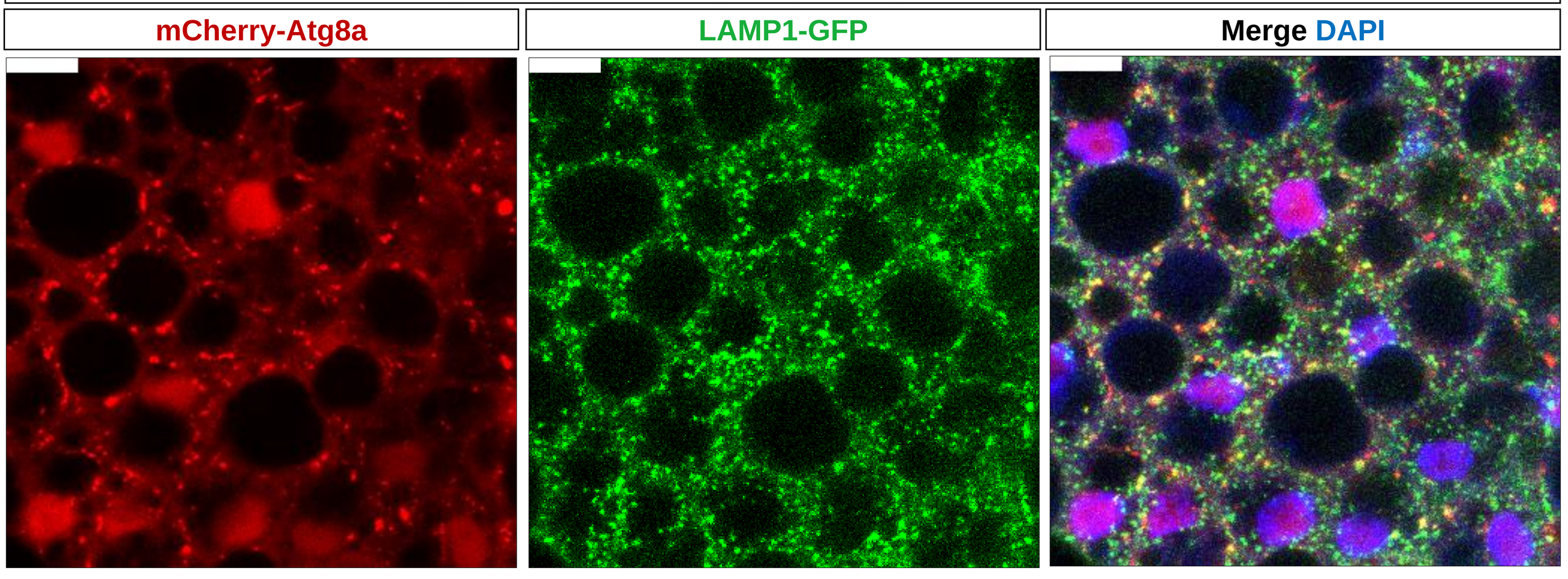

C Genomic rescue of *wacky* programmed autophagy phenotype

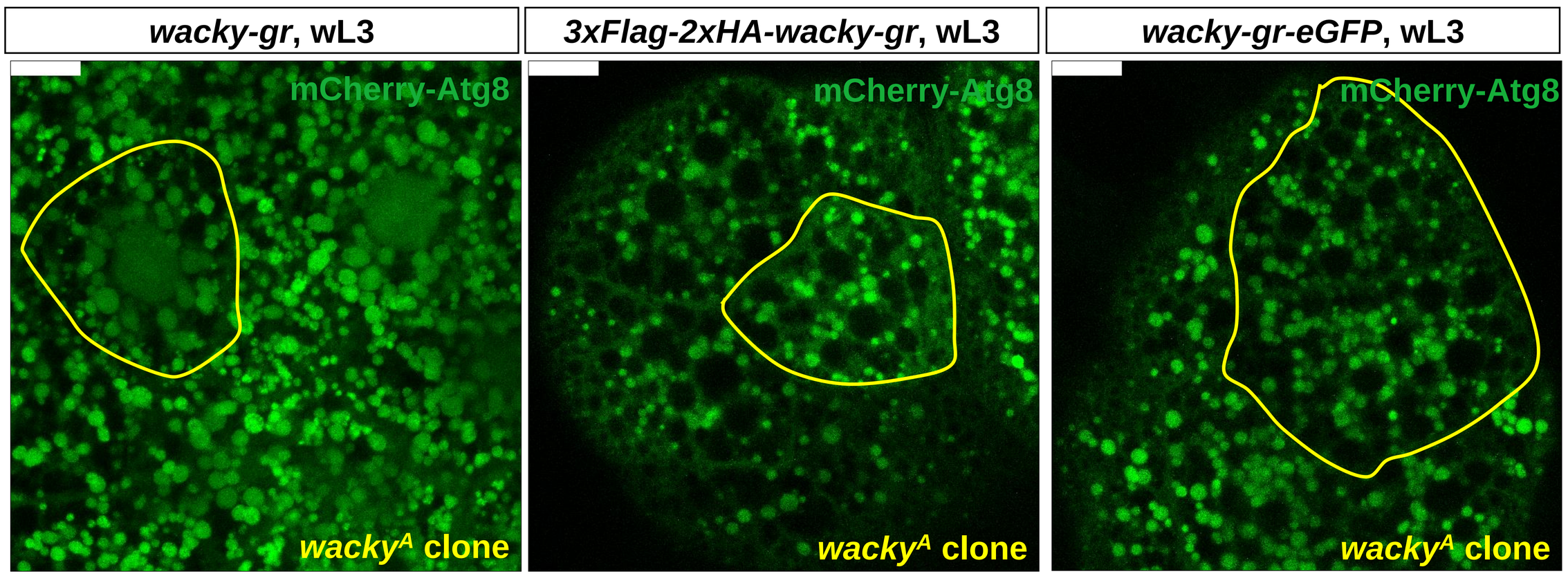

Figure S3

A *wacky*^{A} exhibits decrease in dTOR activity

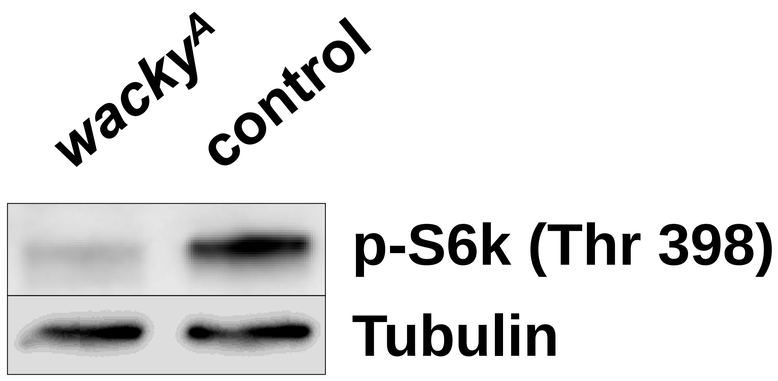

B dTOR overexpression suppresses the autophagy phenotype of *wacky* mutant clones in the fat body

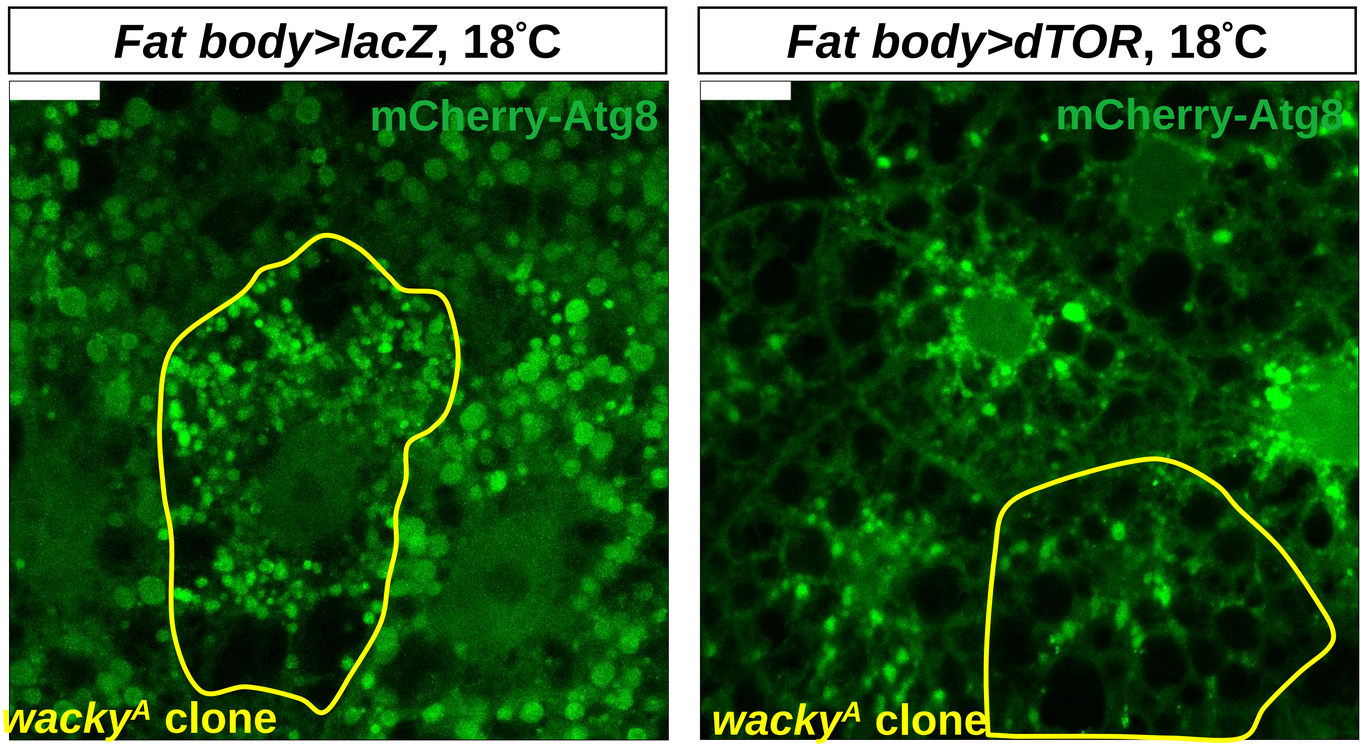

C dTOR overexpression decreases *wacky*^{A} autophagic vesicles and lysosomes in *Drosophila* retina and improves synaptic transmission

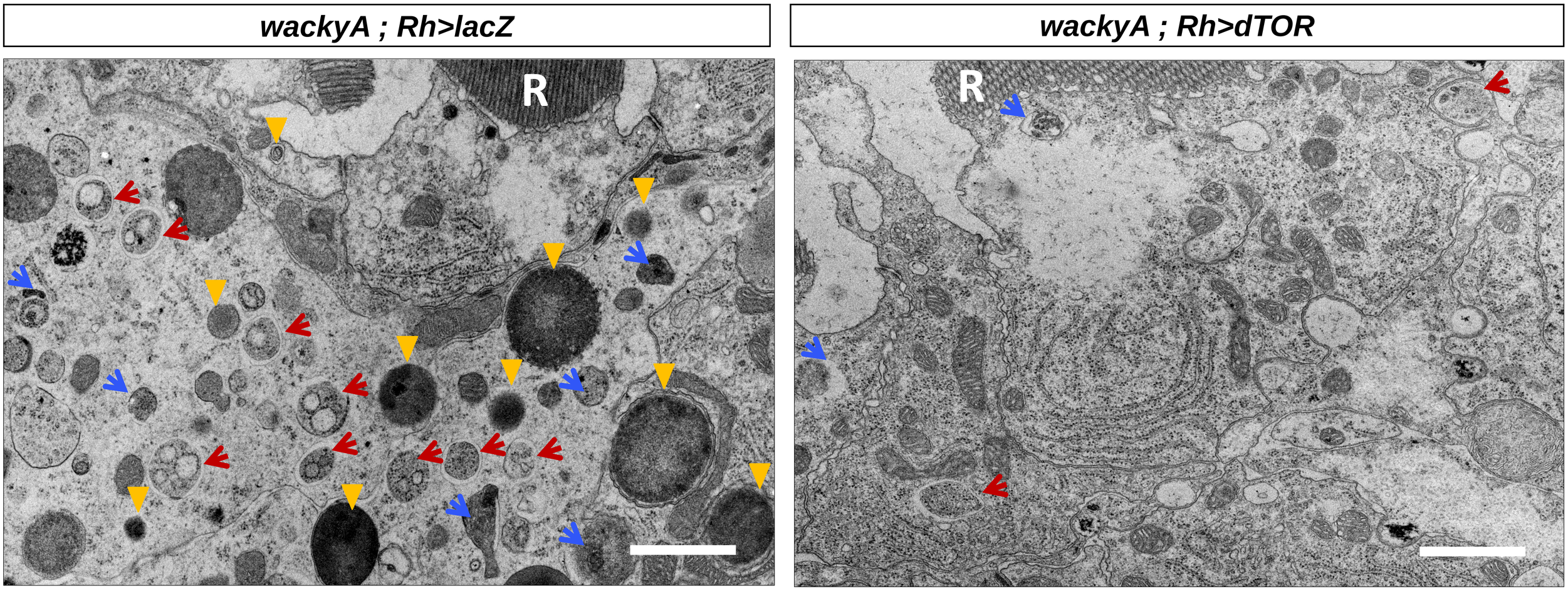

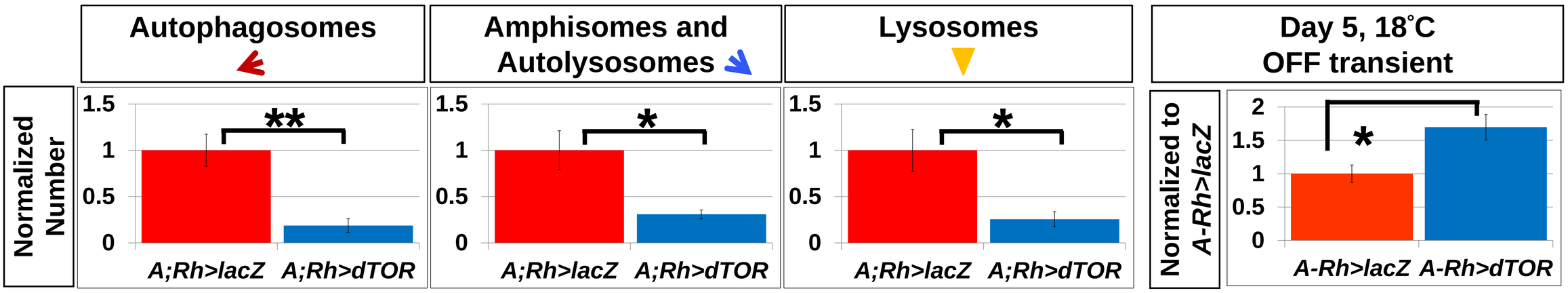

D Quantification of clone size

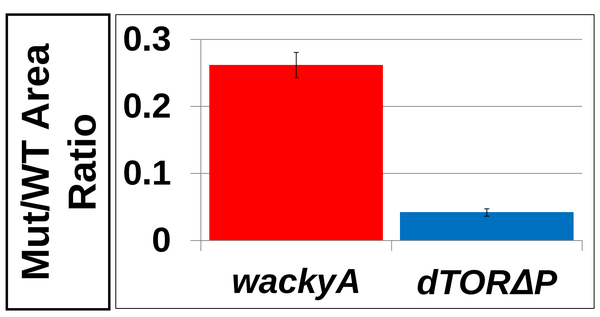

E Quantification of cell size

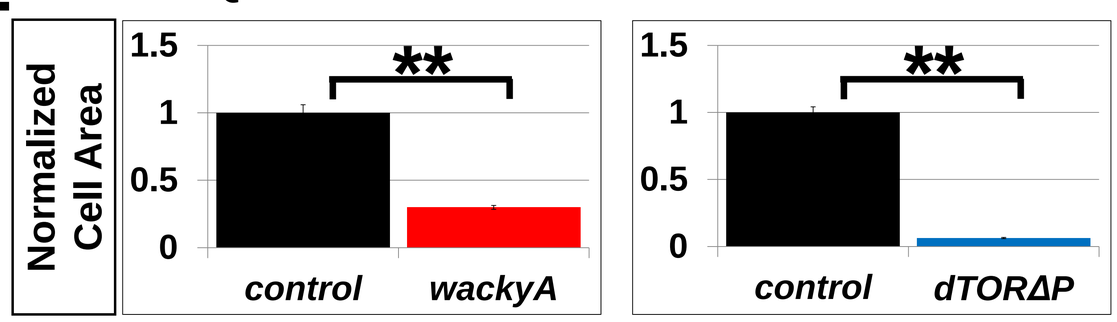

Figure S4

A Loss of WAC increases basal autophagy in HeLa and SH-SY5Y cells

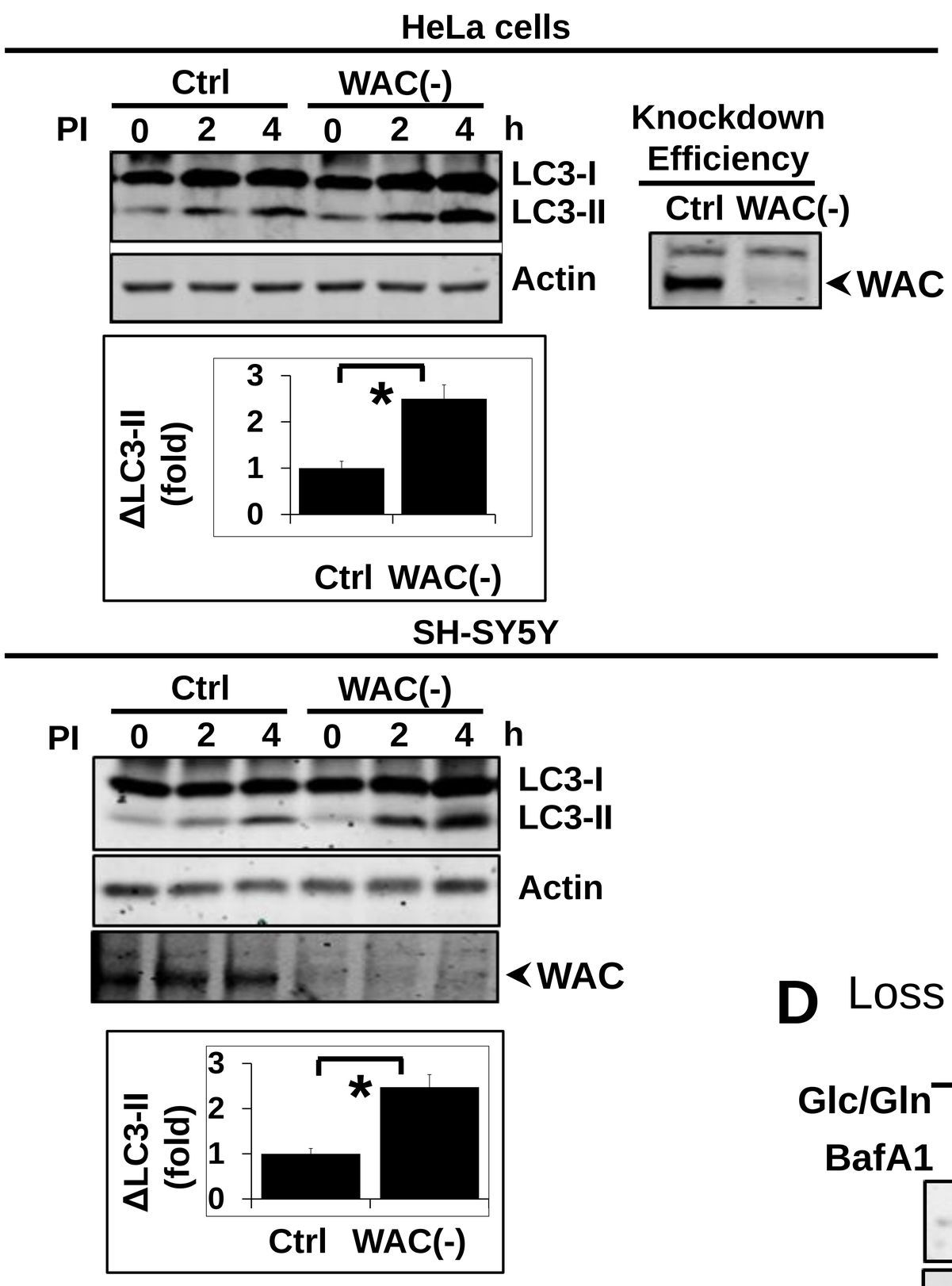

B Knocking down ATG7 restores basal autophagy levels

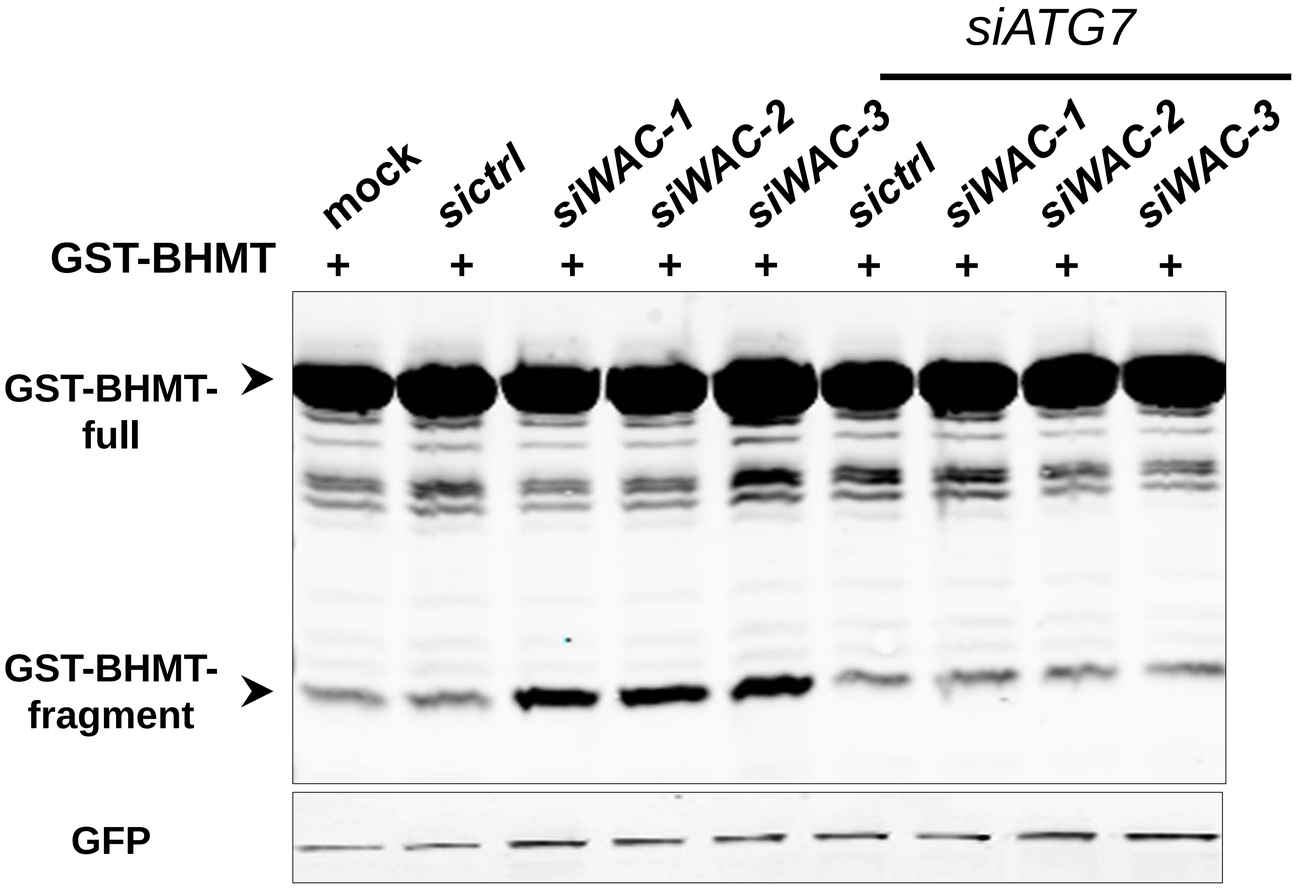

C WAC interaction with mTOR pathway components is conserved in basal conditions

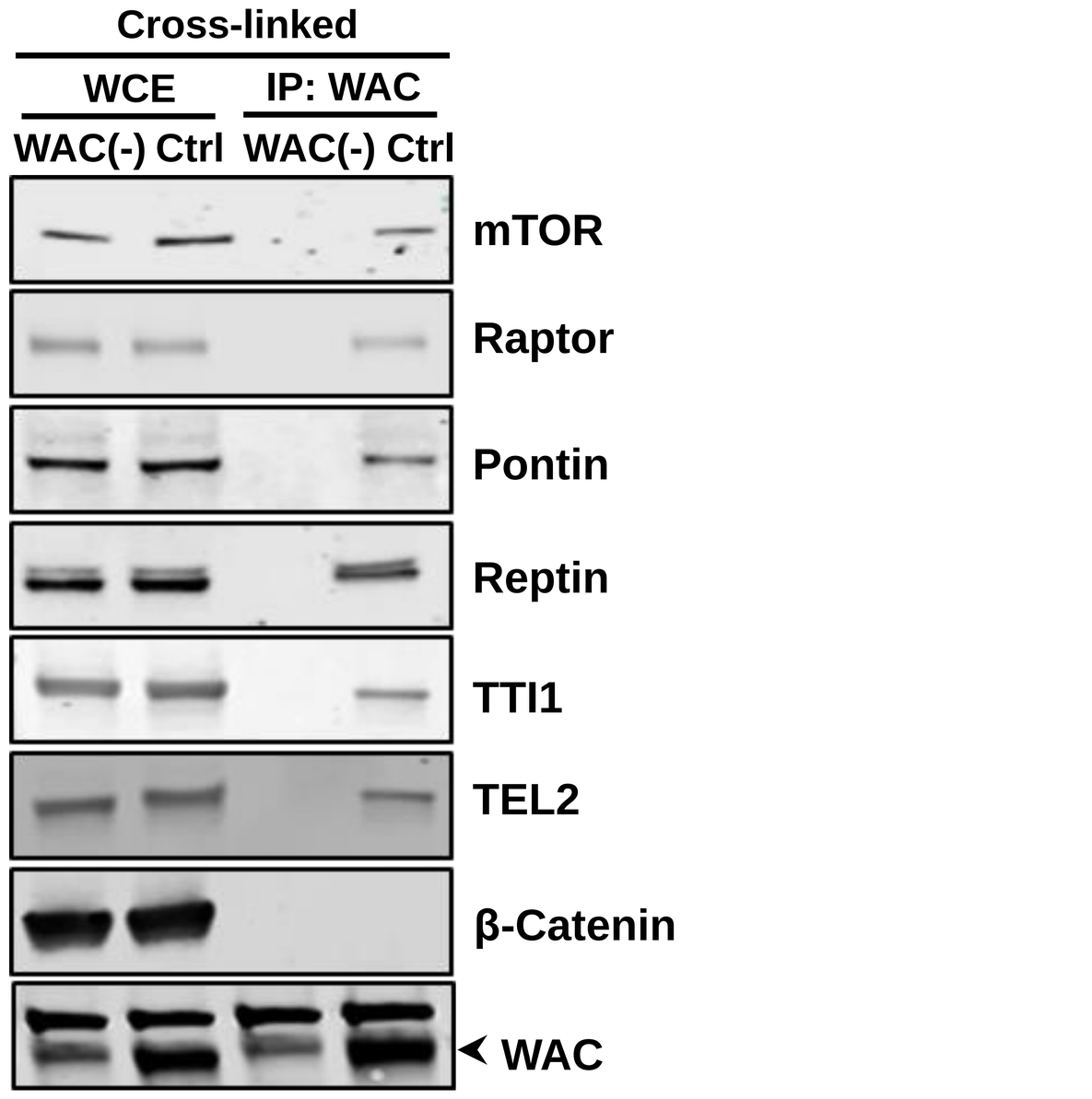

D Loss of WAC decreases p62 levels

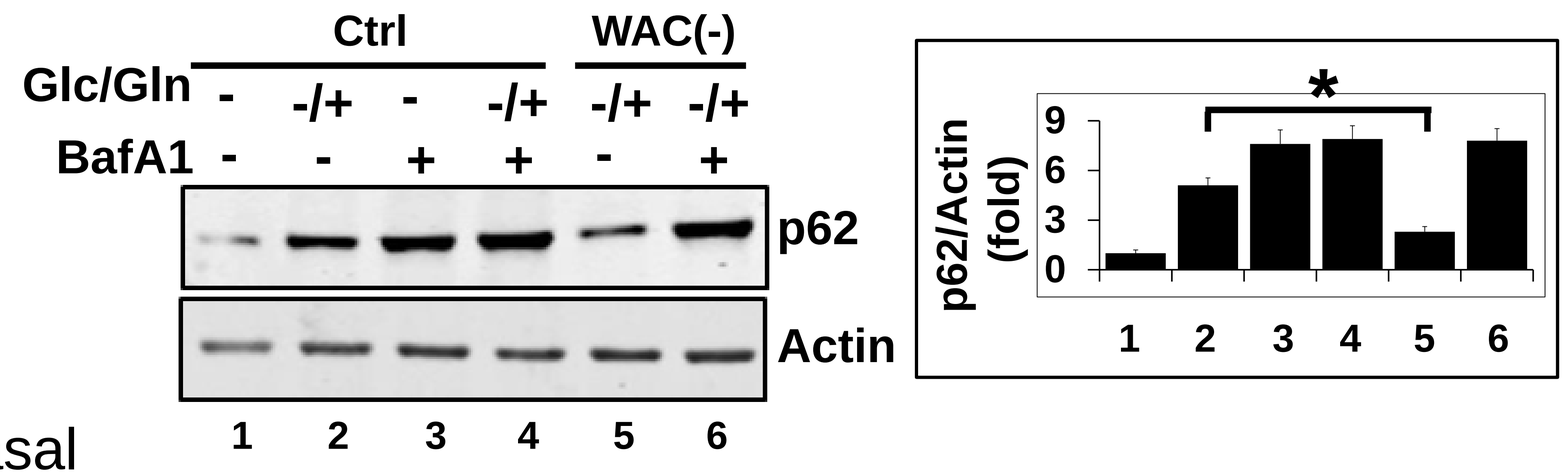

E Loss of WAC increases LC3-II levels

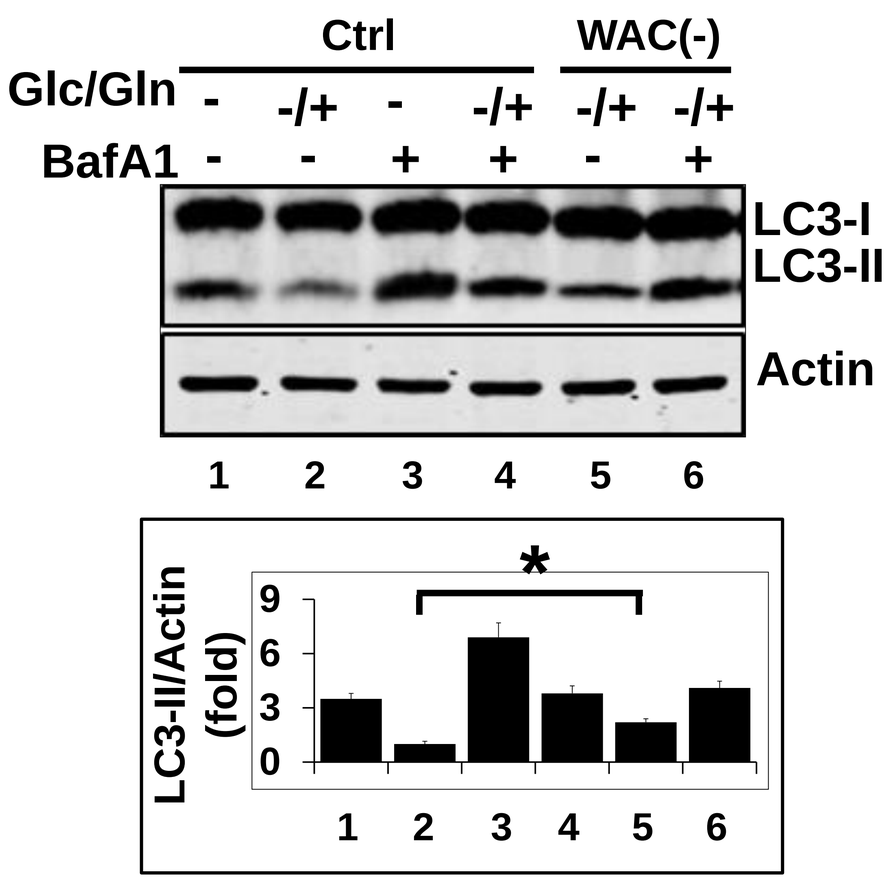

Figure S5

A

Loss of WAC reduces TTT binding to Pontin/Reptin in SH-SY5Y cells

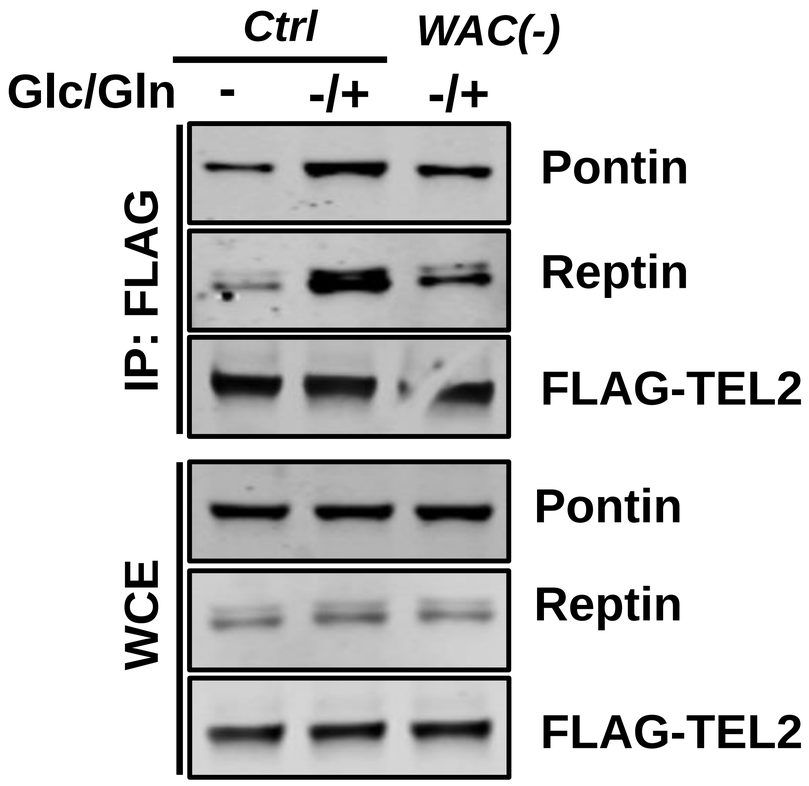

B

Quantification for Figure 6E

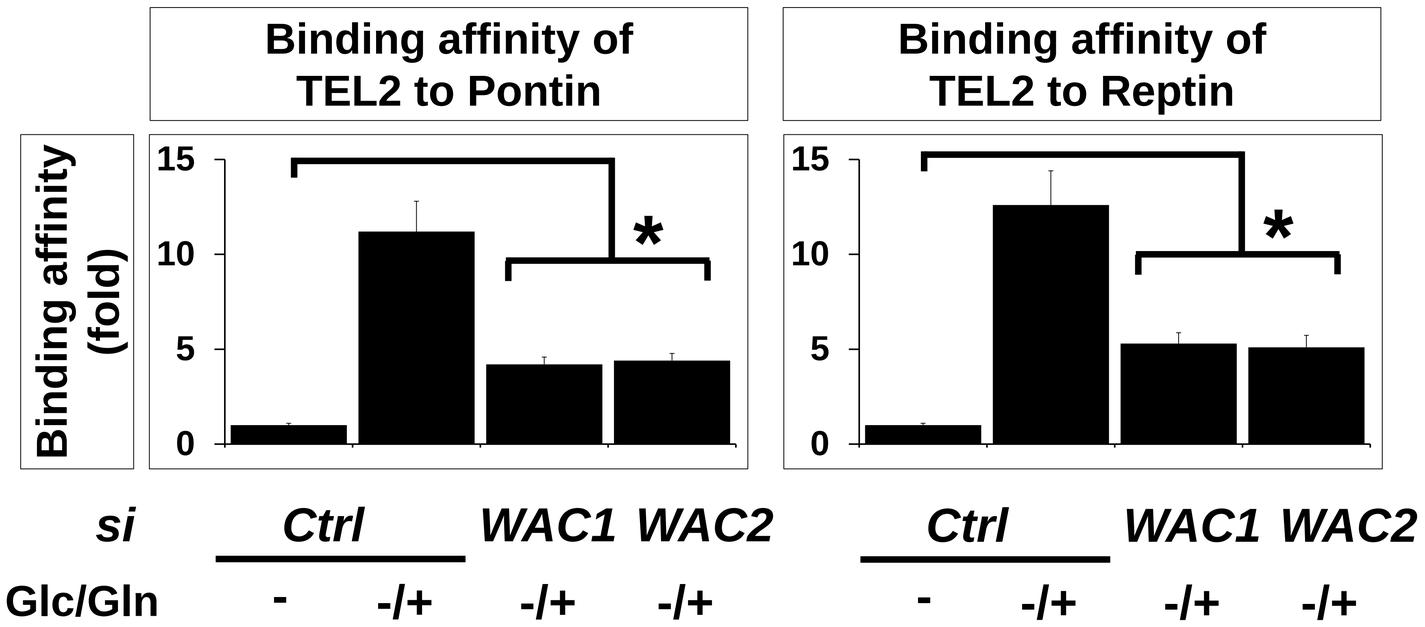

C

Quantification for Figure 6F

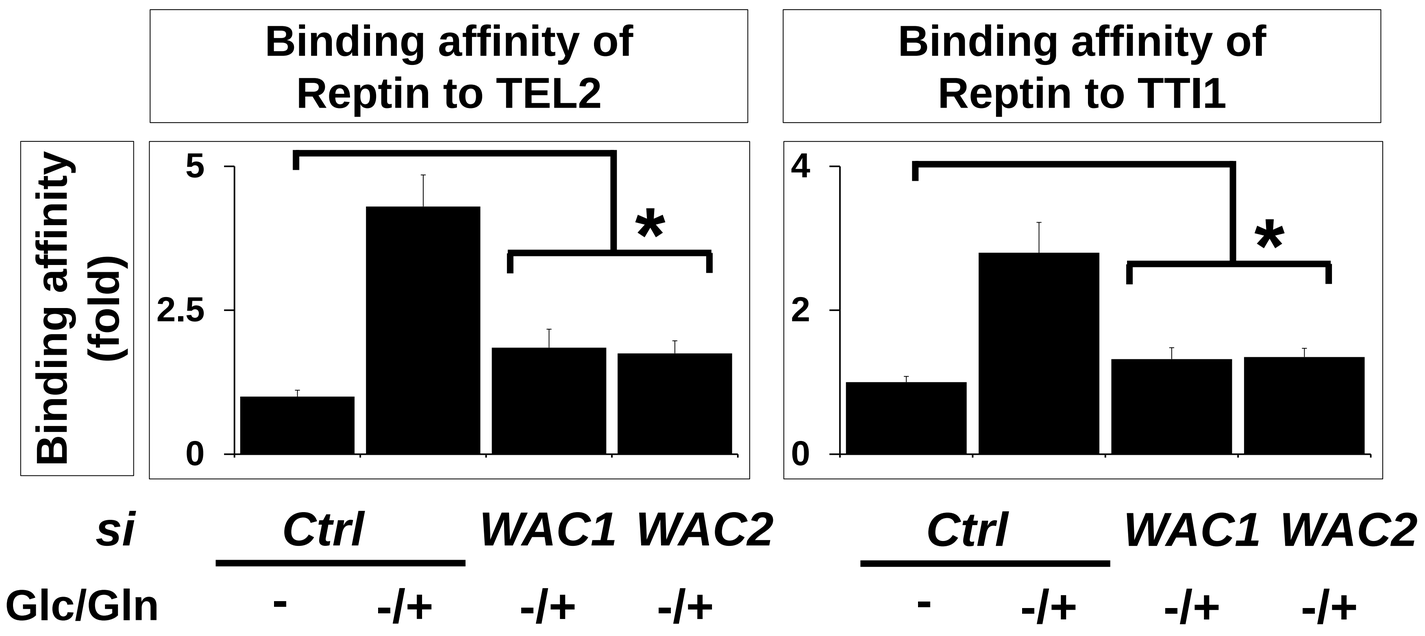

Figure S6

A

Quantification for Figure 7A

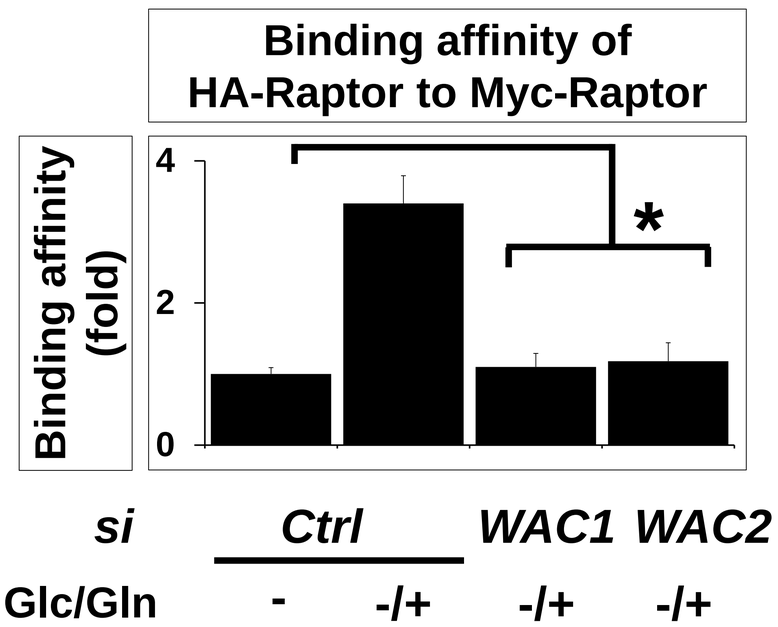

B

Quantification for Figure 7B

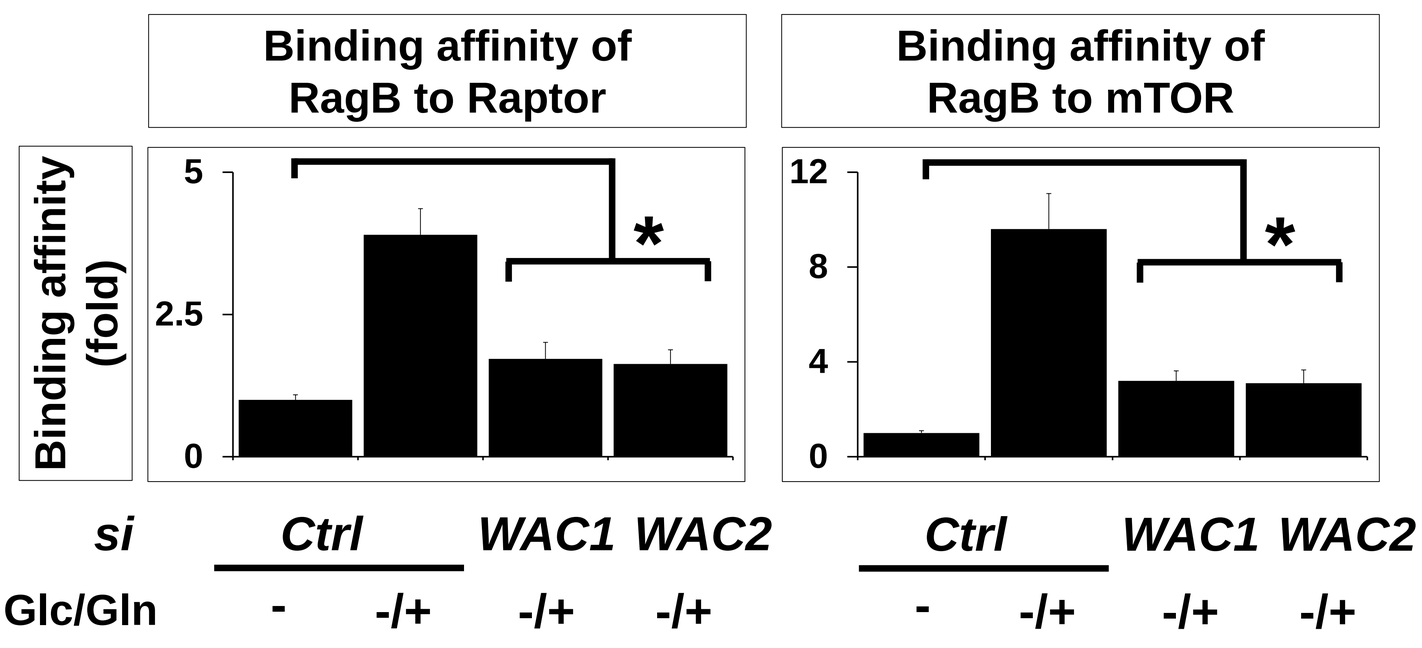

C

Loss of WAC affects PIKK stability
in HEK293T cells

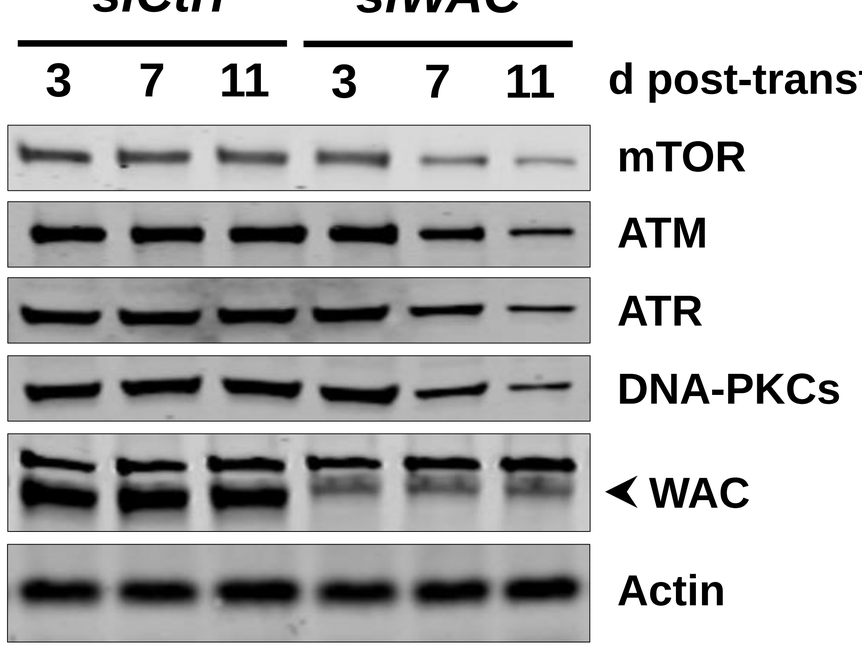

Figure S7

SUPPLEMENTAL FIGURE LEGENDS

Figure S1 (Related to Figure 1). *XE14* alleles affect neuronal survival and basal autophagy

(A) A simplified diagram of how mTORC1 senses energy status, growth factors, and amino acids. Positive regulation (arrow), negative regulation (blocked line).
(B) TEM images of the retina of ey-FLP clones of control (*y w FRT19A*) and $XE14^{C}$ raised in 12-hour light/12-hour dark cycle, at 1 day old and 36 days old. Scale bars are 2 µm.
(C) TEM images of the lamina of ey-FLP clones of control (*y w FRT19A*) (n=3), $XE14^{A}$ (n=3), and $XE14^{C}$ (n=3), raised in 12-hour light/12-hour dark cycle, at 1 day old and 36 days old, with quantification of autophagic vesicles for 36-day old lamina. In the central cartridge of 1 day old control, the photoreceptor terminals are marked blue and the epithelial glia are marked magenta. Scale bars are 1 µm, error bars are SEM, and ** is $p<0.02$.

Figure S2 (Related to Figure 2). The morphological and functional phenotypes of *wacky* mutants are rescued by genomic Wacky transgenes, which are broadly expressed in adult and larval tissues

(A) TEM images of the retina of ey-FLP clones of $wacky^{A}$ and $wacky^{A}$ with genomic *wacky* transgene, at 5 days old, showing rescue of morphological defects. Scale bars are 2µm.
(B) ERG traces from 19-day old ey-FLP clones of $wacky^{A}$ and $wacky^{A}$, $wacky^{B}$, and $wacky^{C}$ with genomic *wacky* transgenes, showing rescue of ERG defects.
(C) Western blot with anti-HA of adult and larval tissues from $wacky^{A}$ rescued with *3xFLAG-2x-HA*-tagged genomic w*acky* transgene.
(D) Immunofluorescence with anti-HA of larval tissues from $wacky^{C}$ rescued with *3xFLAG-2x-HA*-tagged genomic *wacky* transgene. Scale bars are 40 µm.

Figure S3 (Related to Figure 3). Starvation-induced autophagy and autophagosome-lysosome fusion in the absence of *wacky*, and genomic rescue of *wacky* autophagy phenotypes

(A) $wacky^{A}$ clones in starved early third instar larval fat body are marked by yellow lines. *Cg-GAL4*-driven expression of *UAS-mCherry-Atg8a* and *LAMP1-GFP* shows decreased numbers of autophagosomes and lysosomes in $wacky^{A}$ clones compared to surrounding control cells. *wacky* genomic rescue (gr) transgene rescues the phenotype. Scale bars are 20 µm.
(B) $wacky^{A}$ second instar larval fat bodies co-expressing *UAS-mCherry-Atg8a* and *UAS-LAMP1-GFP* with the fat body-specific *Cg-GAL4* driver show co-localization of mCherry-Atg8a and LAMP1-GFP . Scale bars are 10 µm.
(C) The autophagy phenotype of $wacky^{A}$ clones, marked by yellow lines, in wandering third instar larval fat body is rescued by genomic rescue (gr) transgenes for untagged genomic *wacky*, *3xFLAG-2xHA*-tagged genomic *wacky*, and *EGFP*-tagged genomic *wacky*. Scale bars are 20 µm.

Figure S4 (Related to Figure 4). dTOR activity and dTOR overexpression in $wacky^{A}$

(A) (A)Western blot of protein lysates from the fat body of second instar larval $wacky^{A}$; *wacky-gr* (control) and $wacky^{A}$ shows decreased dTOR-dependent phosphorylation of S6k.
(B) *Cg-GAL4*-driven expression of *UAS-lacZ* as control or *UAS-dTOR* in fat body with $wacky^{A}$ clones shows that *wacky* autophagy phenotype is suppressed by overexpression of dTOR. Scale bars are 20 µm.
(C) *Rh1-GAL4*-driven expression of *UAS-lacZ* (n=3) as control or *UAS-dTOR* (n=3) in $wacky^{A}$ retina clones shows that *wacky* autophagy and synaptic transmission phenotypes are suppressed by overexpression of dTOR. R stands for rhabdomere. Scale bars are 1 µm. Error bars are SEM, **$p<0.02$, and *$p<0.05$.
(D) Quantification for clone size in Figure 4E as ratio of mutant clone area/control twin spot area. Error bars are SEM, **$p<0.02$.

(E) Quantification for cell size in Figure 4F as cell area normalized to control cell area. Error bars are SEM, **p<0.02.

Figure S5 (Related to Figure 5). Human WAC regulates autophagy and interacts with mTORC1 and the TTT-Pontin/Reptin complex

(A) Basal autophagy is assayed in HeLa and SH-SY5Y cells by monitoring LC3-II synthesis with or without lysosomal protease inhibitor (PI). WAC knock down increases LC3-II levels, indicating an increase in basal autophagy. ΔLC3-II is calculated as the difference between LC3-II levels at 4 hours and 2 hours after PI treatment. Error bars are SEM , n=3, and * p<0.05.
(B) Basal autophagy is assayed in HEK 293T cells by monitoring the autophagy-dependent fragmentation of the GST-BHMT reporter. WAC knock down increases the level of fragmented GST-BHMT (GST-BHMT fragment), indicating an increase in basal autophagy, and treatment with siRNA against an essential autophagy gene, ATG7, suppresses this increased basal autophagy.
(C) Immunoprecipitation with WAC antibody under basal unstimulated conditions. Endogenous WAC interactions with endogenous mTOR, Raptor, and TTT-Pontin/Reptin are evident with cross-linking in HEK293T cells. WCE, Whole cell extract.
(D) Glucose/glutamine depletion (-) followed by repletion (-/+) induces (D) accumulation of p62 and (E) a decrease in the level of LC3-II. These energy-dependent responses are inhibited by WAC knock down. Bafilomycin treatment shows that translation of p62 and LC3 is not compromised with loss of WAC. Error bars are SEM, n=3, and * p<0.05.

Figure S6 (Related to Figure 6). WAC promotes the assembly of the TTT-Pontin/Reptin complex

(A) In SH-SY5Y cells treated with glucose/glutamine depletion (-) followed by glucose/glutamine repletion (-/+), WAC knock down (WAC(-)) decreases the interaction of TTT and Pontin/Reptin, as shown by co-IP with anti-FLAG-TEL2.
(B) Quantification of the reduction of TEL2 binding to Pontin and Reptin upon WAC knock down (n=3). The non-specific band above WAC is the loading control. Error bars are SEM, n=3, and *p<0.05.
(C) Quantification of the reduction of Reptin binding to TEL2 and TTI1 upon WAC knock down (n=3). The non-specific band above WAC is the loading control. Error bars are SEM, n=3, and *p<0.05.

Figure S7 (Related to Figure 7). WAC facilitates mTORC1 dimerization and mTORC1-RagB interaction

(A) Quantification of the reduction of Myc-Raptor to HA-Raptor upon WAC knock down (n=3). The non-specific band above WAC is the loading control. Error bars are SEM, n=3, and *p<0.05.
(B) Quantification of the reduction of RagB binding to mTOR and Raptor upon WAC knock down (n=3). The non-specific band above WAC is the loading control. Error bars are SEM, n=3, and *p<0.05.
(C) In HEK293T cells, prolonged WAC knock down decreases protein levels of the PIKK proteins, mTOR, ATM, ATR, and DNA-PKcs. This is shown through Western blots for PIKK proteins at 3, 7, and 11 days (d) post-transfection with control and WAC siRNA.

Table S1 (Related to Figure 4). Top 30 Interactors and dTOR Pathway Interactors of Wacky

Fly Protein	Human Homologs	Peptide Hits
Bre1	RNF20, RNF40	204
Mhc	MYH6, MYH7	157
ACC	ACACA, ACACB	154
BetaTub85D	TUBB4A	121
Kst	SPTBN5	71
Idh	IDH1, IDH2	57
Cct5	CCT5	40
Moe	MSN	35
Prp8	PRPF8	34
L(1)G0334	PDHA2	32
Mhcl	MYO18A	32
CG3491	SBNO1, SBNO2	31
Trol	HSPG2	29
Syncrip	HNRNPR	29
Hem	NCKAP1	29
CG17687	WDR96	29
Vps13	VPS13A	28
v(2)k05816	FASN	28
Got1	GOT1, GOT2	27
CG2875	NOC4L	26
Smid	NVL	26
Nrx-1	NRXN1, NRXN2, NRXN3	25
LanB1	LAMB1, LAMB2, LAMB4	25
Myo10A	MYO15A	24
Pug	MTHFD1	24
Ect4	SARM1	24
Sli	SLIT1, SLIT2, SLIT3	24
Pfk	PFKM	23
CG8771	NUP188	22
dTOR	**mTOR**	**22**
Wacky (CG8949)	**WAC**	**21**
Rept	**Reptin/RUVBL2**	**15**
Pont	**Pontin/RUVBL1**	**9**
Vha100-2	**ATP6V0A4**	**9**

SUPPLEMENTAL EXPERIMENTAL PROCEDURES

Fly strains and clonal analysis

XE14 alleles were isolated as described in Yamamoto et al., 2014, from a chemical mutagenesis screen on isogenized *y w FRT19A* flies. *XE14* alleles were complemented by *Dp(1;Y)W73* y^{31d} B^{1} f^{+} B^{S} (Eberl et al., 1992) and failed to complement *Df(1)BSC582* (Cook et al., 2012) and *Df(1)ED7374* (Ryder et al., 2007), narrowing the region of interest to four genes. Mutations in *wacky* (*CG8949*) were identified through Sanger sequencing. *Cg-Gal4*, *da-Gal4*, *Act-Gal4*, *rh1-Gal4*, *P{Ubi-mRFP.nls}1* w^{*} *P{hsFLP}12 P{neoFRT}19A; P{UASp-mCherry-Atg8a}2* (Nezis et al., 2009), *UAS-lacZ*, *UAS-rag*^{Q61L} (Kim et al., 2008), *UAS-Atg1-RNAi* (Ni et al., 2009), *UAS-Rheb.Pa* (Patel and Tamanoi, 2006), *UAS-TOR.WT* (Hennig and Neufeld, 2002), *Tor*$^{\Delta P}$ *P{neoFRT}40A* (Zhang et al., 2000), *UAS-Raptor-HA* (Wang et al., 2012), and *FRT40A* were obtained from Bloomington *Drosophila* Stock Center, *UAS-Lamp1-GFP* was a gift from Helmut Kramer (Pulipparacharuvil et al., 2005), and *cl(1) P{neoFRT}19A/Dp(1;Y) y+ v+; ey-FLP* was a gift from Drs. John Olson and Utpal Banerjee (Call et al., 2007). All flies were kept at room temperature (~22°C), unless otherwise indicated.

Eye clones were generated by crossing *FRT19A*-containing female flies to *cl(1) P{neoFRT}19A/ Dp(1;Y) y+ v+; ey-FLP or P{GMR-hid}SS1,* y^{1} w^{*} *P{neoFRT}19A; P{GAL4-ey.H}SS5, P{UAS-FLP.D}JD2* and *FRT40A*-containing flies to y^{1} w^{*}*; P{GMR-hid}G1 P{neoFRT}40A, l(2)CL-L*^{1}*/CyO; P{GAL4-ey.H}SS5, P{UAS-FLP.D}JD2*. Fat body clones were generated by crossing *FRT19A*-containing flies to *P{Ubi-mRFP.nls}1* w^{*} *P{hsFLP}12 P{neoFRT}19A*. Eggs laid from 0-6 hours were subjected to a 1-2-hour, 37°C heat shock. Ovary clones were generated as described in Silver and Montell, 2001.

Transmission Electron Microscopy

TEM was performed as previously described (Zhai et al., 2006). Adult heads were dissected and fixed in sodium cacodylate buffer containing 2% paraformaldehyde/2.5% glutaraldehyde and post fixed in aqueous 1% OsO_4. Fixed samples were then dehydrated in an ethanol series, followed by propylene oxide and embedded in EMBED-812 resin (Electron Microscopy Sciences). Plastic sections were stained with 1% uranyl acetate followed by lead citrate before imaging with an electron microscope (1010; JEOL).

Molecular cloning

To generate the *wacky* cDNA construct, the full-length fly *wacky* cDNA was amplified from the LD32364 (Rubin et al., 2000) clone and inserted into the *pUAST-attB* vector by restriction digest and subsequent ligation. To add a C-terminal FLAG-HA tag, the full-length *wacky* cDNA was cloned into a *pUAST-attB* vector with a C-terminal FLAG-HA site.

To generate the human *WAC* cDNA construct, we obtained the *WAC* cDNA from the BC004258 clone (Strausberg et al., 2002). We corrected the C-terminal base pairs by PCR for the translated protein to match the NCBI reference sequence, NP_057712.2. We then inserted the corrected cDNA into the *pUAST-attB* vector by restriction digest and subsequent ligation.

To generate the *wacky* genomic construct, the *wacky* genomic region, with additional 2400 base pairs both upstream and downstream, was obtained from the bacterial artificial chromosome clone, CH321-45K19 (Venken et al., 2009), and cloned into the *P[acman]* vector by recombineering (Venken et al., 2006). An N-terminal 3xFLAG-2xHA tag and a C-terminal EGFP tag were individually added to the *wacky* genomic construct by recombineering, as previously described (Venken et al., 2008).

PRK5-GST-BHMT is a gift from Dr. Patrick B. Dennis (Dennis and Mercer, 2009). FLAG-TEL2 (Kaizuka et al., 2010), HA-Raptor (Kim et al., 2002), Myc-Raptor (Dos et al., 2004), and HA-RagB (Sancak et al., 2008) are from Addgene.

Generation of transgenic flies

Transgenic flies containing *wacky* or human *WAC* cDNA or *wacky* genomic constructs were generated by injecting plasmids into the embryos of *y w;; PBac{y[+]-attP}VK00033* (chromosome III) and *y w; PBac{y[+]-attP}VK00037* (chromosome II) (Venken et al., 2006).

Immunostaining and imaging

Fat body immunostaining protocol was adapted from Pircs et al., 2012. Bisected third instar larvae were inverted and fixed with 4% formaldehyde in PBS overnight at 4°C. Samples were quickly rinsed twice, and washed 2 x 30 minutes in PBS, permeabilized for 15 minutes with PBTX-DOC (PBS with 0.1% Triton X-100 and 0.05% sodium deoxycholate), blocked for 3 hours with 5% donkey serum/PBTX-DOC, incubated overnight at 4°C with mouse monoclonal anti-FLAG (Sigma) in 1% donkey serum in PBTX-DOC, washed 3 x 30 minutes in PBTX-DOC, incubated with the secondary antibody donkey anti-mouse Cy3 conjugate (Jackson ImmunoResearch) in 1% donkey serum/PBTX-DOC for 2 hours, and washed 3 x 15 minutes in PBTX-DOC and 1 x 15 minutes in PBS. Fat bodies were then dissected and mounted in SlowFade®Gold (Life Technologies). Immunostaining of other larval tissues was done by first fixing bisected and inverted larvae with 4% formaldehyde in PBS for 1 hour at room temperature. Samples were washed 2 x 30 minutes with PBT (0.1% TritonX-100 in PBS), blocked for 1 hour in 5% donkey serum/PBT, incubated with mouse anti-HA (Covance) in 5% donkey serum/PBT overnight at 4°C, washed 3 x 15 minutes with PBT, incubated with secondary antibody in 5% donkey serum/PBT for 1 hour, and washed 3 x 15 minutes with PBT. Samples were then dissected and mounted in SlowFade®Gold. Ovariole immunostaining was done as described in Yoon et al., 2011, with mouse anti-DLG (Development Studies Hybridoma Bank) and rabbit anti-GFP (Life Technologies). Images were captured with a Zeiss LSM 710 confocal microscope and analyzed using Image J.

Affinity Purification-Mass Spectrometry

Whole larval protein extracts in lysis buffer [25 mM Tris-HCl, pH 7.4, 150 mM NaCl, 0.5% NP-40, 5% glycerol, 1 mM EDTA and protease inhibitor cocktail (Roche)] were used for immunoprecipitation using GFP-Trap (Chromotek) following manufacturer's instructions. As described in (Zhang et al., 2013), protein samples were boiled with Laemmli buffer and subjected to SDSPAGE [4–20% Tris/glycine gel (Novex; Invitrogen)]. Coomassie brilliant blue–stained protein bands were excised and subjected to in-gel digestion with trypsin as previously described (Jung et al., 2005). Nano-HPLC tandem mass spectrometry analysis of the isolated protein complex using advanced linear ion trap-mass spectrometer (LTQ Orbitrap Velos; Thermo Fisher Scientific) was performed as previously described (Sung et al., 2008). Each tryptic peptide was loaded onto an in-house Reprosil-Pur Basic C18 (3 µm, Dr. Maisch GmbH, Germany) trap column which was 2 cm X 100 µm in size. Then the trap column was washed with loading solution and switched in-line with an in-house 6 cm x 150 µm column packed with Reprosil-Pur Basic C18 equilibrated in 0.1% formic acid/water. The peptides were separated with a 75 min discontinuous gradient of 5-28% acetonitrile/0.1% formic acid at a flow rate of 800 nl/min. Separated peptides were directly electrosprayed into the mass spectrometer using a nanospray source with a voltage of 2.5 kV applied to the liquid junction. The mass spectrometer was operated in the data-dependent mode acquiring fragmentation spectra of the top 35 strongest ions. Obtained tandem mass spectrometry spectra were searched against *Drosophila* RefSeq database from FlyBase (ftp://ftp.flybase.net/genomes/aaa/) with Mascot algorithm (Mascot 2.4, Matrix Science) embedded in Proteome Discoverer 1.4 interface (Thermo Fisher Scientific). The precursor mass tolerance was confined within 10 ppm with fragment mass tolerance of 0.5 D and a maximum of three missed cleavages allowed. Assigned peptides were filtered with 5% false discovery rate and subjected to verifications to eliminate false identification.

***Drosophila* western blotting**

Tissues were homogenized in 2X Laemmli sample buffer (Bio-Rad). Proteins were separated by SDS-PAGE and transferred onto nitrocellulose membrane (Bio-Rad). Antibodies used were mouse monoclonal anti-HA (Covance), Ref(2)P antibody (Rui et al., 2015), Phospho-p70 S6 kinase (Thr 398) antibody (Cell Signaling), S6 kinase antibody (Santa Cruz), Phospho-4E-BP1 (Thr37/46) antibody (Cell Signaling),

Phospho-Akt (Ser505) antibody (Cell Signaling), Akt antibody (Cell Signaling), and alpha-Tubulin antibody (Sigma).

Cell culture and transfection

HEK 293T, HeLa, and SH-SY5Y cells were maintained in DMEM medium (Corning) containing 10% fetal bovine serum, 100 IU penicillin, and 100ug/ml streptomycin. Small interfering RNAs and plasmid DNA were transfected using lipofectamine 2000 (Life Technologies) according to manufacturer's instructions. For glucose/glutamine repletion experiments, cells were first starved with DMEM containing dialyzed FBS (Life Technologies) and lacking glucose/glutamine for 3 hours, then repleted with full medium for 30 mins prior to cell lysis.

RNA interference

The following siRNAs were synthesized by Sigma-Aldrich:

siWAC-1 (CCAGUUACUCUCCACAAGA) (Totsukawa et al., 2011),

siWAC-2 (CCAGUGGAAUGGAAGACAA) (Totsukawa et al., 2011),

siWAC-3 (GAAAGAGAACAGAGACAAA) (Zhang and Yu, 2011),

siATG7 (CCAACACACUCGAGUCUUU) (Lavieu et al., 2006)

siPontin was from Santa Cruz Technology (sc-43543).

Lentivirus-mediated shRNA: Based on the protocols provided by Addgene, lentivirus constructs carrying shRNA against human WAC were generated and delivered to cultured cells upon packaging into replication-deficient lentiviral particles to generate WAC knockdown clones. All the packaging and envelope plasmids including psPAX2 and pMD2.G were obtained from Addgene. The shRNA transfer vector plasmid against WAC was obtained from Sigma Mission Library (gene ID: NM_016628.4; clone TRCN0000138407). Control cells were transduced with lentiviral particles carrying MISSION® pLKO.1 Non-Target shRNA Control Plasmid (Sigma). Knockdown of WAC was tested periodically (each 2-3 months) during the study and representative immunoblots for the absence of the proteins are included in the manuscript.

Co-immunoprecipitation and western blotting

HEK 293T cells in 60-mm dishes were lysed in CHAPS lysis buffer (40 mM HEPES (pH 7.4), 1mM EDTA, 120 mM NaCl, 10 mM β-glycerophosphate, 1 mM NaF, 1 mM Na_3VO_4, and 0.3% CHAPS) supplemented with protease inhibitors (Roche). Lysed cells were briefly sonicated before being centrifuged at 13,000 rpm for 30 minutes at 4°C. For immunoprecipitation, antibodies indicated were incubated with Protein A/G Plus agarose beads (Santa Cruz) and pre-cleared supernatant. Immunoprecipitates or total cell lysates were denatured by 2X SDS sample buffer before western blot analysis. Proteins were transferred to nitrocellulose membranes using Bio-Rad mini transfer apparatus followed by blocking with 5% non-fat milk and primary antibody incubation. Secondary antibodies including IRdye 680RD and IRdye 800CW for the Odyssey western system were from LI-COR Biosciences.

Antibodies used were anti-GST (Santa Cruz), anti-Myc (Santa Cruz), anti-TTI1 (Santa Cruz), Normal rabbit IgG (Santa Cruz), anti-Actin (Millipore), anti-WAC (Millipore), anti-mTOR (Cell Signaling), anti-Raptor (Cell Signaling), anti-Reptin (Sigma), anti-Pontin (Sigma and Cell Signaling), anti-ATM (Cell Signaling), anti-DNA-PK (Cell Signaling), and anti-ATR (Cell Signaling).

SUPPLEMENTAL REFERNCES

Call, G.B., Olson, J.M., Chen, J., Villarasa, N., Ngo, K.T., Yabroff, A.M., Cokus, S., Pellegrini, M., Bibikova, E., Bui, C., et al. (2007). Genomewide clonal analysis of lethal mutations in the *Drosophila melanogaster* eye: Comparison of the X chromosome and autosomes. Genetics *177*, 689–697.

Cook, R.K., Christensen, S.J., Deal, J.A., Coburn, R.A., Deal, M.E., Gresens, J.M., Kaufman, T.C., and Cook, K.R. (2012). The generation of chromosomal deletions to provide extensive coverage and subdivision of the *Drosophila melanogaster* genome. Genome Biol. *13*, R21.

Dos, D.S., Ali, S.M., Kim, D.H., Guertin, D.A., Latek, R.R., Erdjument-Bromage, H., Tempst, P., and Sabatini, D.M. (2004). Rictor, a novel binding partner of mTOR, defines a rapamycin-insensitive and raptor-independent pathway that regulates the cytoskeleton. Curr. Biol. *14*, 1296–1302.

Eberl, D.F., Perkins, L.A., Engelstein, M., Hilliker, A.J., and Perrimon, N. (1992). Genetic and developmental analysis of polytene section 17 of the X chromosome of *Drosophila melanogaster*. Genetics *130*, 569–583.

Jung, S.Y., Malovannaya, A., Wei, J., O'Malley, B.W., and Qin, J. (2005). Proteomic analysis of steady-state nuclear hormone receptor coactivator complexes. Mol. Endocrinol. *19*, 2451–2465.

Kim, D.H., Sarbassov, D.D., Ali, S.M., King, J.E., Latek, R.R., Erdjument-Bromage, H., Tempst, P., and Sabatini, D.M. (2002). mTOR interacts with raptor to form a nutrient-sensitive complex that signals to the cell growth machinery. Cell *110*, 163–175.

Lavieu, G., Scarlatti, F., Sala, G., Carpentier, S., Levade, T., Ghidoni, R., Botti, J., and Codogno, P. (2006). Regulation of autophagy by sphingosine kinase 1 and its role in cell survival during nutrient starvation. J. Biol. Chem. *281*, 8518–8527.

Ni, J.Q., Liu, L.P., Binari, R., Hardy, R., Shim, H.S., Cavallaro, A., Booker, M., Pfeiffer, B.D., Markstein, M., Wang, H., et al. (2009). A *Drosophila* resource of transgenic RNAi lines for neurogenetics. Genetics *182*, 1089–1100.

Pircs, K., Nagy, P., Varga, A., Venkei, Z., Erdi, B., Hegedus, K., and Juhasz, G. (2012). Advantages and Limitations of Different p62-Based Assays for Estimating Autophagic Activity in *Drosophila*. PLoS One *7*, e44214.

Rubin, G.M., Hong, L., Brokstein, P., Evans-Holm, M., Frise, E., Stapleton, M., and Harvey, D.A. (2000). A *Drosophila* Complementary DNA Resource. Science (80-.). *287*, 2222–2224.

Ryder, E., Ashburner, M., Bautista-Llacer, R., Drummond, J., Webster, J., Johnson, G., Morley, T., Yuk, S.C., Blows, F., Coulson, D., et al. (2007). The DrosDel deletion collection: A *Drosophila* genomewide chromosomal deficiency resource. Genetics *177*, 615–629.

Sancak, Y., Peterson, T.R., Shaul, Y.D., Lindquist, R.A., Thoreen, C.C., Bar-Peled, L., and Sabatini, D.M. (2008). The Rag GTPases bind raptor and mediate amino acid signaling to mTORC1. Science *320*, 1496–1501.

Silver, D.L., and Montell, D.J. (2001). Paracrine signaling through the JAK/STAT pathway activates invasive behavior of ovarian epithelial cells in *Drosophila*. Cell *107*, 831–841.

Strausberg, R.L., Feingold, E.A., Grouse, L.H., Derge, J.G., Klausner, R.D., Collins, F.S., Wagner, L., Shenmen, C.M., Schuler, G.D., Altschul, S.F., et al. (2002). Generation and initial analysis of more than 15,000 full-length human and mouse cDNA sequences. Proc. Natl. Acad. Sci. U. S. A. *99*, 16899–16903.

Sung, Y.J., Li, Y., Wang, Y., Chen, Y., Zhao, Y., and Qin, J. (2008). Complications in the assignment of 14 and 28 Da mass shift detected by mass spectrometry as in vivo methylation from endogenous proteins. Anal. Chem. *80*, 1721–1729.

Venken, K.J.T., He, Y., Hoskins, R.A., and Bellen, H.J. (2006). P[acman]: a BAC transgenic platform for targeted insertion of large DNA fragments in D. melanogaster. Science *314*, 1747–1751.

Venken, K.J.T., Kasprowicz, J., Kuenen, S., Yan, J., Hassan, B.A., and Verstreken, P. (2008). Recombineering-mediated tagging of *Drosophila* genomic constructs for in vivo localization and acute protein inactivation. Nucleic Acids Res. *36*, e114.

Venken, K.J.T., Carlson, J.W., Schulze, K.L., Pan, H., He, Y., Spokony, R., Wan, K.H., Koriabine, M., de Jong, P.J., White, K.P., et al. (2009). Versatile P[acman] BAC libraries for transgenesis studies in *Drosophila melanogaster*. Nat. Methods *6*, 431–434.

Yoon, W.H., Meinhardt, H., and Montell, D.J. (2011). miRNA-mediated feedback inhibition of JAK/STAT morphogen signalling establishes a cell fate threshold. Nat. Cell Biol. *13*, 1062–1069.

Zhai, R.G., Cao, Y., Hiesinger, P.R., Zhou, Y., Mehta, S.Q., Schulze, K.L., Verstreken, P., and Bellen, H.J. (2006). *Drosophila* NMNAT maintains neural integrity independent of its NAD synthesis activity. PLoS Biol. *4*, e416.